Copyright © 2000, by the author(s).
All rights reserved.

Permission to make digital or hard copies of all or part of this work for personal or classroom use is granted without fee provided that copies are not made or distributed for profit or commercial advantage and that copies bear this notice and the full citation on the first page. To copy otherwise, to republish, to post on servers or to redistribute to lists, requires prior specific permission.

KINETICS OF PHOTORESIST ETCHING IN A LARGE AREA PLASMA SOURCE (LAPS)

by

Kazushige Takechi and Michael A. Lieberman

Memorandum No. UCB/ERL M00/40

1 August 2000

KINETICS OF PHOTORESIST ETCHING IN A LARGE AREA PLASMA SOURCE (LAPS)

by

Kazushige Takechi and Michael A. Lieberman

Memorandum No. UCB/ERL M00/40

1 August 2000

ELECTRONICS RESEARCH LABORATORY

College of Engineering
University of California, Berkeley
94720

Kinetics of Photoresist Etching in a Large Area Plasma Source (LAPS)

Kazushige Takechi[1] and M. A. Lieberman[2]

[1]*Visiting Industrial Fellow, NEC Corporation in Japan*

[2]*Department of Electrical Engineering and Computer Sciences*

University of California at Berkeley

Berkeley, CA 94720

ABSTRACT

We report on photoresist etching experiments on the large area plasma source (LAPS) with an oxygen plasma. The etch rate rises to a maximum value and then falls with increasing gas pressure. Using a recently proposed etching model, this experimental result can be explained in terms of a simplified discharge kinetics model as well as our previous simulation results.

We find that the etching uniformity over the processing area of 40 cm$\times$50 cm decreases with increasing gas pressure. This can be explained by the experimental plasma profile results and our simulation results in which the plasma density profile becomes more non-uniform with increasing gas pressure. We also find that the standing wave pattern along the antenna coil can strongly influence etch process uniformity.

1. Introduction

We have developed a simplified oxygen discharge model corresponding to our large area plasma source (LAPS) geometry.[1] For a specified gas pressure and absorbed power, we solved the particle and energy balance equations to predict the ion and O-atom densities and profiles and the electron temperature. Here we report on photoresist etching experiments on the LAPS with an oxygen plasma. The etch rate rises to a maximum value and then falls with increasing gas pressure. A simplified etch kinetics model is described in which the predicted ion and O-atom densities are used to explain the etch rate data. In order to gain an insight into the underlying physical mechanism, we also compare the etch rate data with the scaling behavior of the etch rate from a simplified analytical discharge kinetics model.

2. Experiments

The LAPS system used in these experiments has been described previously.[2] For the measurements of photoresist etch rate, half of a four-inch silicon wafer with 2 μm (as measured by ellipsometry) of hardbaked photoresist was clamped at the center and (for uniformity measurements) at the edges of the processing area (40 cm $\times$ 50 cm). Typical operating parameters are an oxygen gas pressure of between 1 mTorr and 100 mTorr and a rf power of between 500 W and 1500 W. No external bias was applied to the wafer during these experiments. The thickness of photoresist film removed was divided by the etch time to determine the etch rate. We assumed that the etch rate was constant over the etch interval. For these etching conditions, we also measured the plasma density profiles, and identified the achievement of launching a traveling wave using four voltage sensors equally spaced along the antenna coil. To launch a traveling wave, the tuning network was adjusted so that the voltages from the four sensors were the same.

3. Results

Plasma density was determined from measurements of the ion saturation current with a Langmuir probe approximately 5 cm in front of the substrate holder. Figure 1 shows plasma density profiles for various oxygen gas pressures at an input power of 500 W. The eight vertical dashed lines in the figure indicate the positions of the eight copper rods. The plasma density profiles are close to symmetric about the center and the plasma density increases with increasing gas pressure. We also see that the density profiles at high pressures (50 mTorr and 100 mTorr) are somewhat embedded with the antenna pattern, which consists of four sets of two adjacent antenna rods each, connected in series in a

serpentine configuration. The plasma density has the peaks within the regions between each of the sets of two copper rods connected in parallel.

Figures 2 and 3 show plasma density profiles for various rf input powers at a gas pressure of 5 mTorr and 50 mTorr, respectively. For both pressures, the plasma density increases roughly linearly with the input power.

We next describe how the etch rate of photoresist changes depending on the oxygen gas pressure and rf input power. Figure 4 shows the etch rate at the center of the substrate holder as a function of both gas pressure and rf input power. The etch rate rises to a maximum value and then falls with increasing gas pressure. The etch rate is clearly a nonlinear function of gas pressure. In order to explain the data in Fig. 4, an etch model proposed by Joubert *et al.*,[3] along with our simulation results and analytical scalings for the discharge kinetics, will be introduced in the next section.

In Fig. 5, the etch rate is plotted along a vertical line (perpendicular to the antenna rods) within the chamber, for gas pressures of 1, 5, 20, and 50 mTorr at an input power of 1000 W. We see that the uniformity of the etch rate decreases with increasing gas pressure. This result can be explained by our simulation results[1] for the ion fluxes to the substrate holder.

Figure 6 shows etch rate profiles along the vertical within the chamber, for a traveling wave condition and standing wave condition at a gas pressure of 20 mTorr. The corresponding voltage distributions along the antenna are shown in the inset. As seen in the figure, the profile for the standing wave condition is highly asymmetric and non-uniform. From this result, we see that the standing wave pattern can strongly influence etch process uniformity.

4. Discussion

We consider a simple model of photoresist etching to explain the etch rate data at the center of the substrate holder.

The form of the rate expression proposed by Joubert *et al.*[3] is

$$E = K\frac{(\kappa p_O)(\sigma_S \eta j_i)}{\kappa p_O + \sigma_S \eta j_i} \qquad (1)$$

where E is the etch rate, K is a rate coefficient, p_O is the O-atom partial pressure, κ is the thermodynamic adsorption constant for O atoms on the photoresist, σ_S is the density of adsorption sites for O atoms, η is an ion-induced desorption rate constant, and j_i is the ion current to the wafer substrate. In order to obtain values for the constants in Eq. (1), we use the simulation results for O-atom density at the substrate surface ($n_{O\text{-}sub}$) and the flux of ions incident on the substrate ($\Gamma_{i\text{-}sub} = n_{i\text{-}sub}u_B$).[1]

Since p_O is proportional to $n_{O\text{-sub}}$, p_O can be redefined as

$$p_O = p_{O(ref)} \frac{n_{O-sub}}{n_{O-sub(ref)}} = p_{O(ref)} C_1 \qquad (2)$$

Similarly, since j_i is proportional to $\Gamma_{i\text{-sub}}$, j_i can be redefined as

$$j_i = j_{i(ref)} \frac{\Gamma_{i-sub}}{\Gamma_{i-sub(ref)}} = j_{i(ref)} C_2 \qquad (3)$$

It is convenient to rearrange Eq. (1) into the following form[4)]

$$\frac{C_1 C_2}{E} = \frac{C_1}{K\alpha_2} + \frac{C_2}{K\alpha_1} \qquad (4)$$

where α_1 is the product $\kappa p_{O(ref)}$ and α_2 is the product $\sigma_S \eta j_{i(ref)}$. We assume that σ_S, η, and κ are constant for different gas pressures and rf powers. Taking $n_{O\text{-sub}}$ and $\Gamma_{i\text{-sub}}$ at 20 mTorr, 500 W as the reference values, we have

$$\frac{\dfrac{n_{O-sub}}{7.05\times10^{13}} \dfrac{\Gamma_{i-sub}}{1.93\times10^{15}}}{E} = \frac{n_{O-sub}}{7.05\times10^{13}} \frac{1}{K\alpha_2} + \frac{\Gamma_{i-sub}}{1.93\times10^{15}} \frac{1}{K\alpha_1} \qquad (5)$$

Using the etch rates for 20 mTorr and 1 mTorr at 500 W in Fig. 4, we have the following simultaneous equations with respect to $1/K\alpha_2$ and $1/K\alpha_1$.

$$\frac{1}{48.5(\text{nm/min})} = \frac{1}{K\alpha_2} + \frac{1}{K\alpha_1} \quad \text{at 20 mTorr}$$

$$\frac{\dfrac{3.26\times10^{12}}{7.05\times10^{13}} \dfrac{4.27\times10^{15}}{1.93\times10^{15}}}{22.4(\text{nm/min})} = \frac{3.26\times10^{12}}{7.05\times10^{13}} \frac{1}{K\alpha_2} + \frac{4.27\times10^{15}}{1.93\times10^{15}} \frac{1}{K\alpha_1} \quad \text{at 1 mTorr}$$

This equation yields values of 1.89×10^{-2} min/nm for $1/K\alpha_2$ and 1.72×10^{-3} min/nm for $1/K\alpha_1$. Figure 7 shows the etch rate data as a function of both gas pressure and rf input power, and the predicted etch rate from Eq. (5) with the above two constants and the simulation results for 1, 5, 20, 50, and 100 mTorr taken from reference 1. Here we have also assumed that $n_{O\text{-sub}}$ and $\Gamma_{i\text{-sub}}$ are proportional to rf power. This assumption seems to be reasonable from the experimental results in Figs. 2 and 3. Equation (5) predicts a somewhat lower rate than the experimental data for a high rf power of 1500 W, but does predict the general trend.

Equation (5) is also used to predict vertical etch rate profiles for various gas pressures, using the simulation results for vertical $n_{O\text{-sub}}$ and $\Gamma_{i\text{-sub}}$ profiles taken from reference 1. The results are shown in Fig. 8. For a gas pressure of 5 mTorr, Eq. (5) predicts a somewhat steeper profile than the experimental result in Fig. 5, but the general trends are similar, with the uniformity decreasing with increasing

pressure. The somewhat steeper etch profiles at 5 mTorr could be explained in terms of the metal-surface recombination coefficient for O atoms ($\gamma_{O\text{-}metal}$). We have taken $\gamma_{O\text{-}metal}$ = 0.1 in the simulation.[1] If we took a lower value as the recombination coefficient, the O-atom density profile would become flatter, resulting in a more uniform etch profile.

We next discuss the etch rate behavior in Fig. 4 in terms of a simplified discharge kinetics and its scalings. The discharge power balance at the substrate holder can be written

$$P_{sub} = A_{sub} e E_T n_{i-sub} u_B \qquad (6)$$

where P_{sub} is the power dissipation at the substrate holder, A_{sub} is the substrate holder area (60 cm×70 cm), and E_T is the total energy lost per electron-ion pair created.[5] The ion flux to the substrate is determined from Eq. (6) as

$$\Gamma_{i-sub}(n_{O_2}) = n_{i-sub} u_B = \frac{P_{sub}(n_{O_2})}{e A_{sub} E_T(n_{O_2})} \qquad (7)$$

As has been seen in the simulation results,[1] both P_{sub} and E_T depend on the gas pressure n_{O2}. The ion flux $\Gamma_{i\text{-}sub}$ thus also varies with n_{O2} as seen in Eq. (7).

For the production of O atoms by dissociation of the oxygen feedstock, the steady-state rate equation is[5]

$$A_{sub} l \frac{dn_O}{dt} = 2A_{sub} l K_{diss} n_i n_{O_2} - \gamma_{sub} 2A_{sub} \frac{1}{4}\overline{v}_O n_{O-sub} = 0 \qquad (8)$$

where l is a discharge thickness.

Solving Eq. (8) for $n_{O\text{-}sub}$,

$$n_{O-sub} = \frac{2l}{\gamma_{sub} 2 \frac{1}{4}\overline{v}_O} K_{diss} n_i n_{O_2} \qquad (9)$$

and using $n_i \approx n_{i\text{-}sub}/h_l$, with $n_{i\text{-}sub}$ given by Eq. (7), we have

$$n_{O-sub}(n_{O_2}) = \frac{2l}{\gamma_{sub} 2 \frac{1}{4}\overline{v}_O e A_{sub}} \frac{K_{diss}(n_{O_2}) P_{sub}(n_{O_2}) n_{O_2}}{u_B(n_{O_2}) E_T(n_{O_2}) h_l(n_{O_2})} \qquad (10)$$

where h_l, a ratio of edge-to-center density, can be expressed as[6]

$$h_l = \frac{0.86}{\left[3 + \frac{l}{2\lambda_i} + \left(\frac{0.86 l u_B}{\pi D_a}\right)^2\right]^{\frac{1}{2}}} \qquad (11)$$

This general h_l factor can be used for transitions from low to high pressure. Since K_{diss}, P_{sub}, u_B, E_T, and

h_l depend on the gas pressure, $n_{O\text{-}sub}$ also is a complicated function of gas pressure as seen in Eq. (10). The values that depend on the gas pressure are summarized in Table 1.

Table 1

p (mTorr)	λ_i (cm)	u_B (cm/s)	D_a (cm^2/s)	T_e (V)	K_{diss} (cm^3/s)	E_T (V)	h_l	n_{O2} (cm^{-3})	P_{sub}/P_{abs}
1	3.0	3.21×10^5	5.10×10^6	3.40	8.1×10^{-10}	120	0.34	3.3×10^{13}	0.58
5	0.61	2.83×10^5	7.95×10^5	2.65	5.1×10^{-10}	200	0.18	1.7×10^{14}	0.56
20	0.15	2.67×10^5	1.76×10^5	2.35	3.9×10^{-10}	260	0.073	6.6×10^{14}	0.44
50	0.061	2.62×10^5	6.80×10^4	2.27	3.6×10^{-10}	290	0.035	1.7×10^{15}	0.30
100	0.030	2.61×10^5	3.38×10^4	2.25	3.5×10^{-10}	300	0.017	3.3×10^{15}	0.20

Using the scaling Eqs. (1), (7), and (10), with the values in Table 1, we predicted the etch rate in the same way as has been done with the simulation results. Figure 9 shows the results. The result from the simplified discharge kinetics model is also in good agreement with the experimental data.

We consider the scaling behavior of the etch rate from Eqs. (1), (7), and (10). In the low pressure regime (low p_O), from Eq. (1), a linear relationship between the etch rate and p_O can be observed. The etch rate therefore increases linearly with $n_{O\text{-}sub}$ defined in Eq. (10). From Eq. (10) with the values in Table 1, $n_{O\text{-}sub}$ increases with gas pressure (n_{O2}), resulting in an increase in the etch rate with gas pressure, as seen in Fig. 9. On the other hand, in the high pressure regime (high p_O), a linear relationship between the etch rate and j_i can be observed. The etch rate is thus proportional to $\Gamma_{i\text{-}sub}$ defined in Eq. (7). From Eq. (7) with the values in Table 1, $\Gamma_{i\text{-}sub}$ decreases with gas pressure (n_{O2}), leading to a decrease in the etch rate with increasing pressure, as seen in Fig. 9.

The fact that both the simulation and analytical discharge kinetics results are in good agreement with the experimental data confirms the assumptions of the model.

5. Conclusions

From the photoresist etching experiments on the LAPS with an oxygen plasma, we have found that the etch rate rises to some maximum value and then falls with increasing gas pressure. Using a recently proposed etching model, the experimental result can be explained in terms of the analytical scalings for discharge kinetics as well as our previous simulation results. This agreement confirms the validity of the various approximations in our model.

For the etching uniformity, we have found that the uniformity over the processing area of 40 cm $\times$ 50

cm decreases with increasing gas pressure. This result can be explained by the experimental results and our simulation results in which the plasma density profile becomes more non-uniform with increasing gas pressure. We also have found that the standing wave pattern along the antenna coil can strongly influence etch process uniformity.

The maximum etch rates were limited to between 100 – 150 nm/min due to power supply and vacuum pumping limitations. We expect the maximum etch rate to increase linearly with rf power. For a large photoresist area, in the O-atom flux limited regime where the etch rate is proportional to $n_{O\text{-}sub}$, we will undergo a reduction in the etch rate due to the loading effect. To minimize the loading effect, high gas flow rates will be required, leading to a reduction in depletion of etchant O atoms over the substrate area.

Acknowledgments

We would like to thank S. Parsa and T. Wang of the UCB Microfabrication Laboratory for providing the wafers and assistance for the measurements of the photoresist thickness. This work was partially supported by National Foundation Grant ECS – 9820836 and the State of California UC – SMART Program under Contract 97 – 01.

References

1) K. Takechi and M. A. Lieberman, An oxygen discharge model for a large area plasma source (LAPS), Memorandum UCB/ERL M00/33, Electronics Research Laboratory, University of California, Berkeley, (2000).

2) K. Takechi and M. A. Lieberman, Operation of a large area plasma source (LAPS) with oxygen gas, Memorandum UCB/ERL M00/15, Electronics Research Laboratory, University of California, Berkeley, (2000).

3) O. Joubert, J. Pelletier, and Y. Arnal, The etching of polymers in oxygen-based plasmas: A parametric study, J. Appl. Phys. 65(12), 5096-5100 (1989).

4) D. A. Carl, D. W. Hess, and M. A. Lieberman, Kinetics of photoresist etching in an electron cyclotron resonance plasma, J. Appl. Phys. 68(4), 1859-1865 (1990).

5) M. A. Lieberman and A. J. Lichtenberg, *Principles of Plasma Discharges and Materials Processing*, John Wiley & Sons Inc., 605 Third Avenue, New York, NY, (1994).

6) C. Lee and M. A. Lieberman, Global model of Ar, O_2, Cl_2, and Ar/O_2 high-density plasma discharges, J. Vac. Sci. Technol. A 13(2), 368-380 (1995).

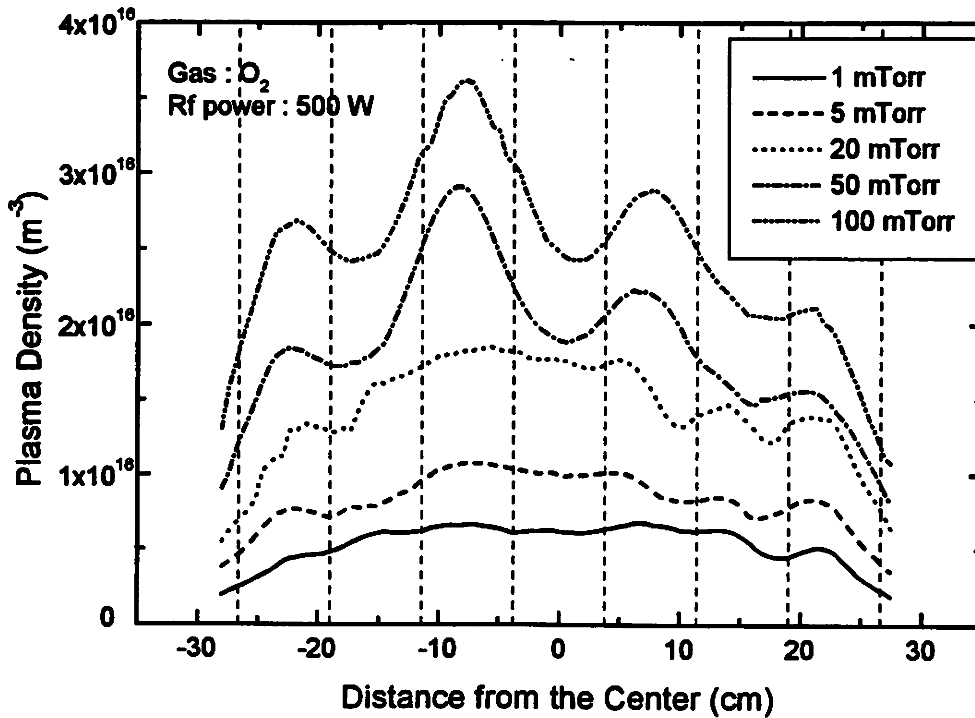

Fig. 1. Plasma density profiles for various oxygen gas pressures at an input power of 500 W.

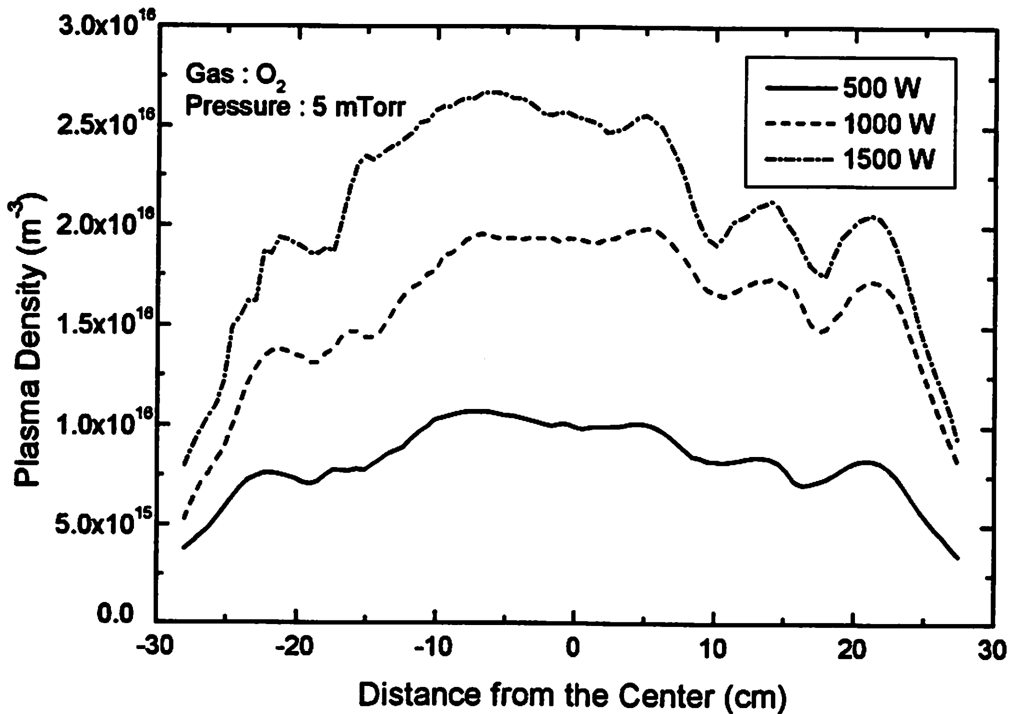

Fig. 2. Plasma density profiles for various rf powers at a gas pressure of 5 mTorr.

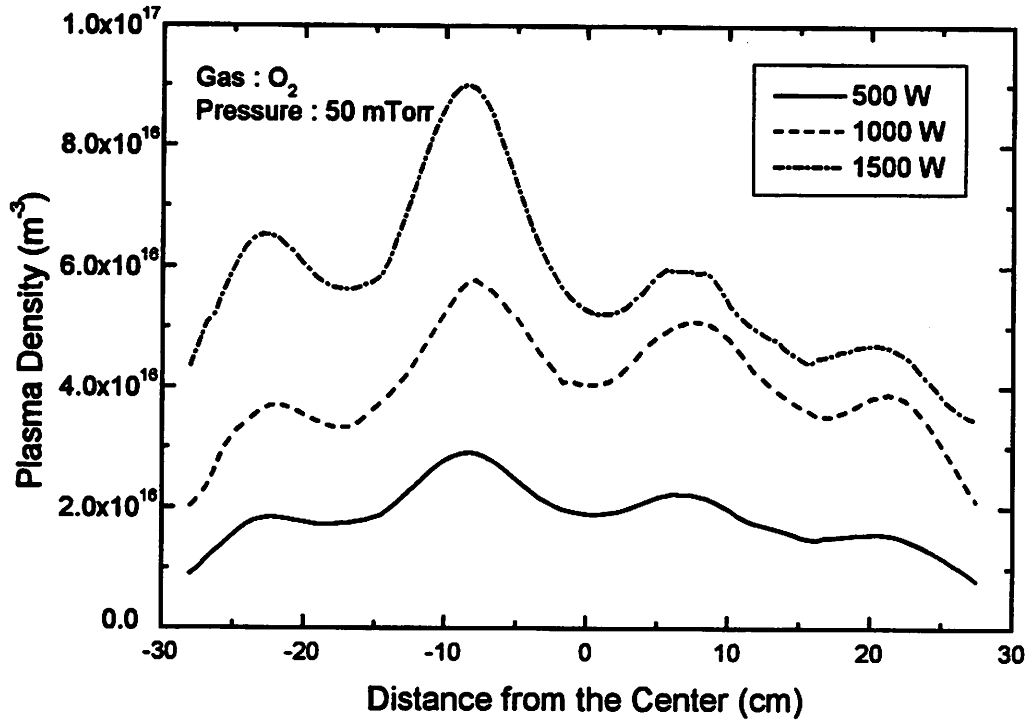

Fig. 3. Plasma density profiles for various rf powers at a gas pressure of 50 mTorr.

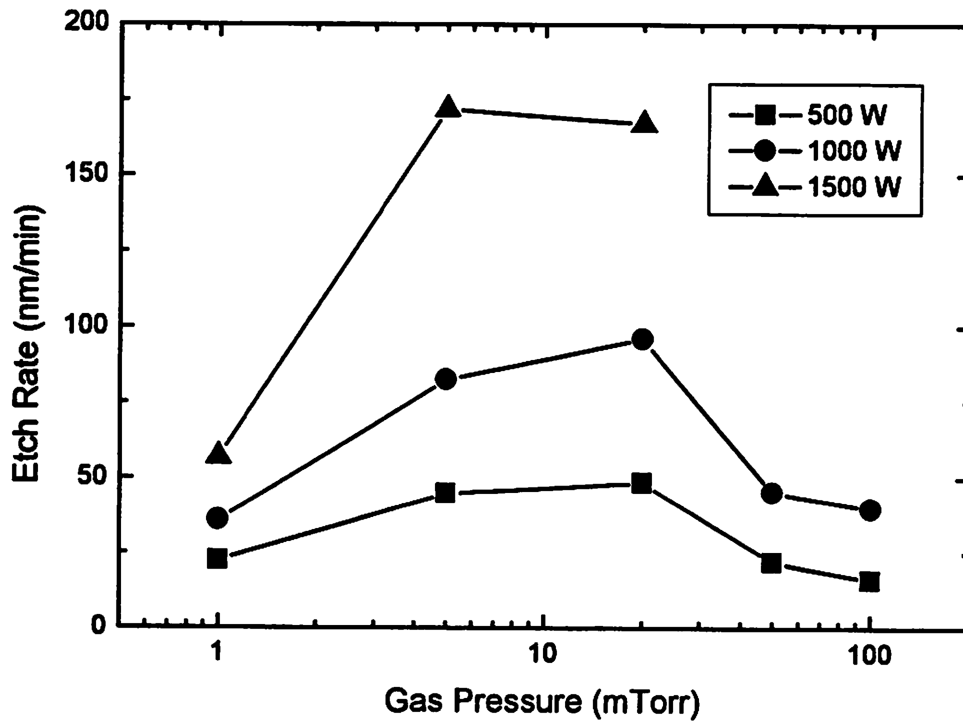

Fig. 4. Dependence of etch rate at the center of the substrate holder on the gas pressure (experimental data).

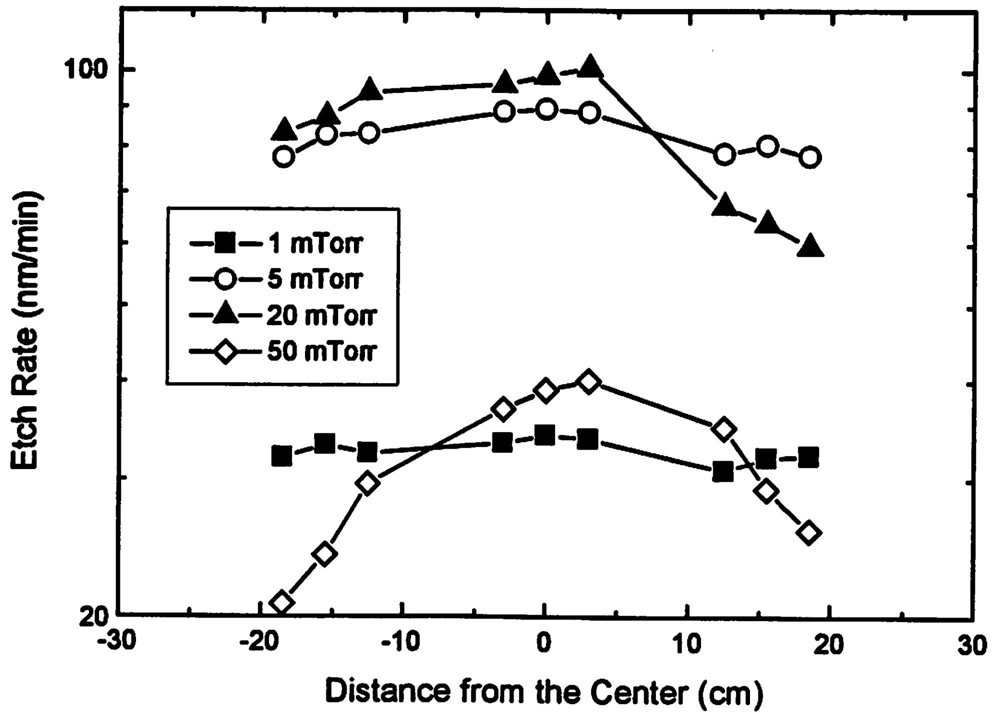

Fig. 5. Vertical etch rate profiles for various gas pressures at an input power of 1000 W.

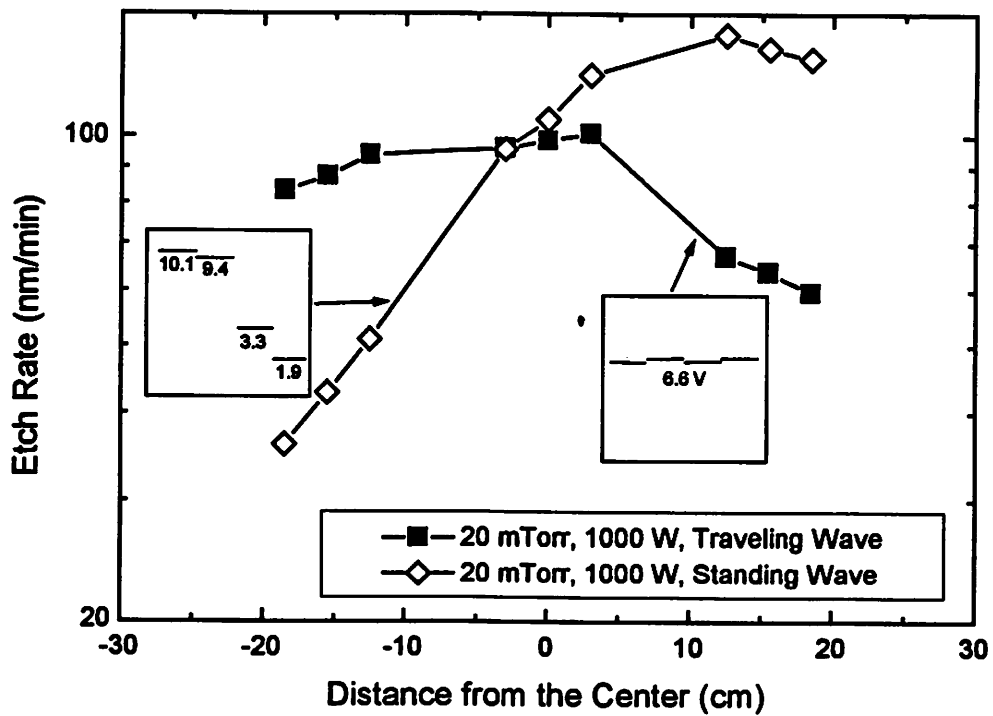

Fig. 6. Vertical etch rate profiles for a traveling wave condition and standing wave condition.

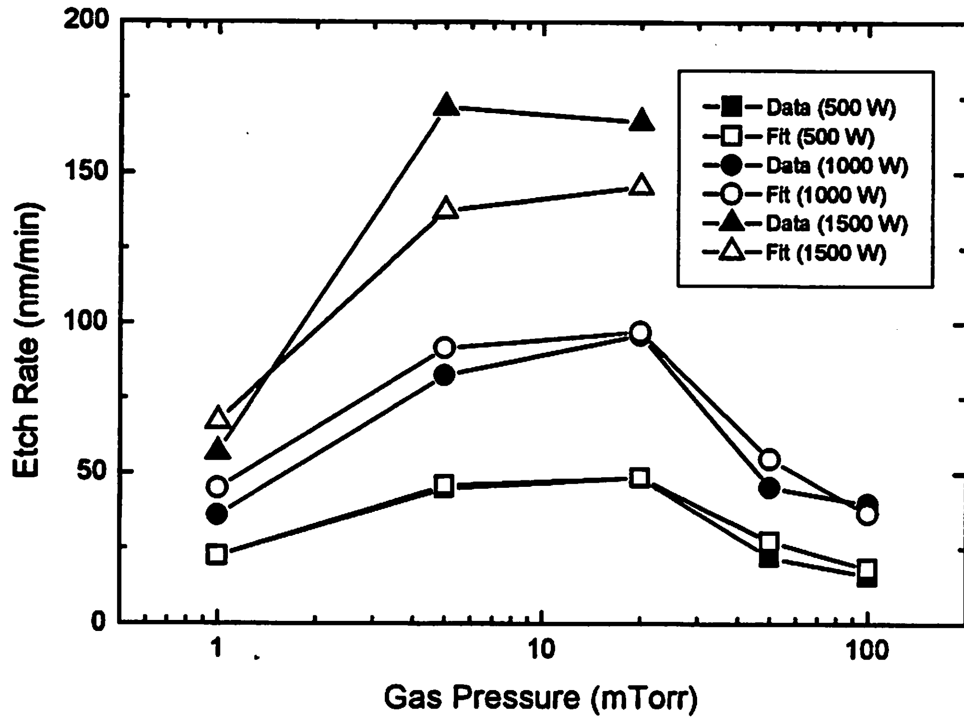

Fig. 7. Plots of etch rate vs gas pressure for various rf powers. The fits are from Eq. (5) with the simulation results.

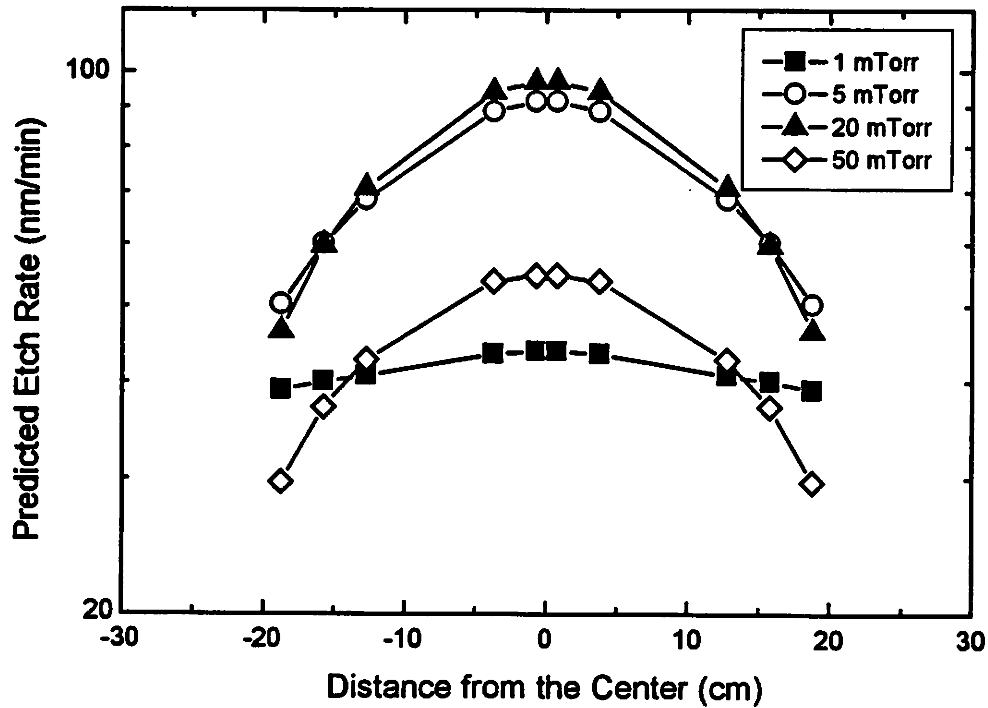

Fig. 8. Predicted vertical etch rate profiles for various gas pressures at 1000 W. The fits are from Eq. (5) with the simulation results.

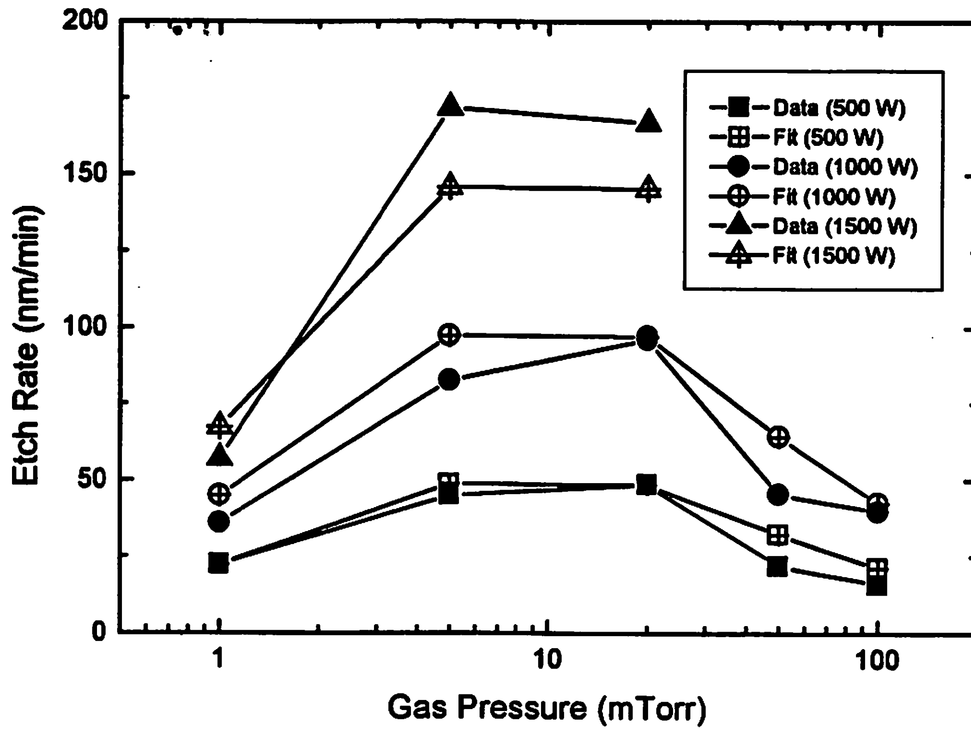

Fig. 9. Plots of etch rate vs gas pressure for various rf powers. The fits are from the scaling Eqs. (1), (7), and (10).